Powder Metallurgy Progress, Vol.21 (2021), No.1, p.018-026
http://dx.doi.org/10.2478/pmp-2021-0003

# SYNTHESIS OF Fe-BASED ALLOY REINFORCED WITH CHROMIUM CARBIDE VIA SINTERING OF IRON-FERROCHROME POWDER MIXTURE

**Yevheniia Kyryliuk, Gennadii Bagliuk, Alla Mamonova, Vitaliy Maslyuk**

***Abstract***
*The results of the investigation of the structure, phase composition, and properties of the alloy sintered from a mixture of iron (65 %) and high-carbon ferrochrome (35 %) powders are presented in the article. It was shown that sintering of the consolidated specimens results in a substantially heterogeneous structure consisting of two predominant phases: austenitic phase and double ferrochrome carbide. A mechanism is proposed for the dissolution of ferrochrome particles in the iron matrix as follows: M7C3 → M3C (1000÷1150 ºC) → M7C3 (1200÷1250 ºC).*
***Keywords: powder, sintering, iron, ferrochrome, composite, phase composition, carbide***

## INTRODUCTION

Among the materials manufactured by powder metallurgy methods, wearproof materials occupy a significant place. The main requirement for ensuring high wear resistance of such materials is the need to create a heterogeneous structure consisting of a relatively soft matrix phase and hard inclusions of refractory compounds that significantly exceed the matrix material in terms of hardness [1,2]. It is obvious that it is just powder metallurgy technologies that make it possible to realize the basic conditions for the creation of wear-resistant materials of this type.

One of the promising groups of relatively inexpensive materials of this class is the composites consisting of an iron-based matrix phase with solid inclusions of chromium carbide [3-8]. These materials have shown high efficiency in operating conditions of intense friction, abrasive wear, corrosive environments, elevated temperatures, etc. The technology for their manufacturing involves the operations of joint grinding of steel and chromium carbide powders, compaction of the mixture, and sintering in the presence of a liquid phase [6-8].

In this work, we proposed the technology for the manufacturing of high-chromium heterogeneous sintered alloys, which is based on using high-carbon Fe-Cr master alloy (ferrochrome) powder instead of chromium carbide as a component of the initial powder mixture, which is designed to form a hard phase inclusions in the alloy. It was assumed that as a result of the interaction of the ferrochrome particles with the matrix phase at sintering temperatures, the corresponding carbide phase would be in situ synthesized in the alloy.

The goal of this work was to study the interaction of the mixture components and the features of phase and structure formation during the sintering of compacts from a powder mixture of iron with high-carbon ferrochrome.

Yevheniia Kyryliuk, Gennadii Bagliuk, Alla Mamonova, Vitaliy Maslyuk: Frantsevich Institute for Problems in Materials Science, NAS of Ukrane, Krzhizhanovsky str., 3, Kyiv, Ukraine, 03142

## MATERIALS AND EXPERIMENTAL PROCEDURE

For the experiments, commercial powders of water-atomized Fe (200 μm) (Fig. 1(a)) and high carbon ferrochrome (100÷200 μm), produced by mechanical grinding of lumpy ferrochrome (Fe-Cr) (Fig. 1(b)) were used. Ferrochrome contains 66.2 % Cr, 24.8 % Fe and 8 % (mass.) C.

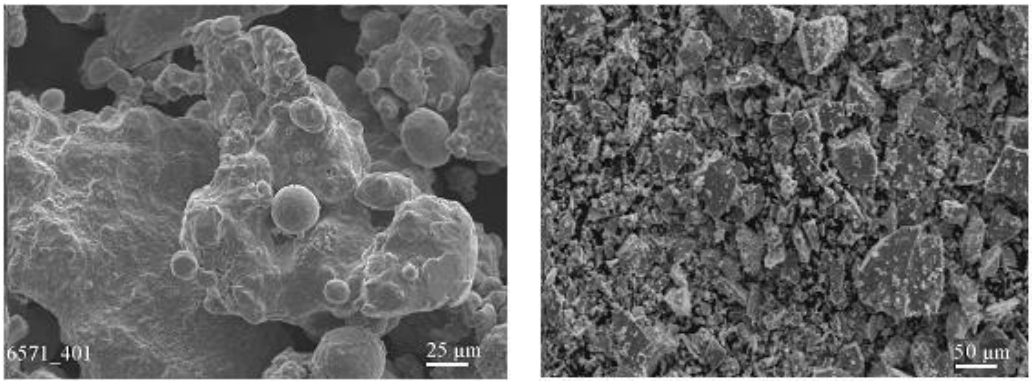
A powder mixture with the ratio of 65% Fe - 35% (Fe-Cr) was prepared by wet ball milling in an alcohol medium, the overall nominal composition thus being Fe-23.2%Cr-2.8%C. Experimental specimens were produced by compaction on a hydraulic press at a pressure of 800 MPa. Samples of cylindrical shape with a size of 10×10 mm were prepared. To determine the physical and mechanical properties, samples in the form of a bar (5× 5×35 mm) were prepared.

Sintering of the samples was carried out in a vacuum furnace in the temperature range of 1000÷1300 °C with isothermal exposure of 30 minutes. The pressure in the vacuum furnace was 1,33 $10^{-2}$ Pa. The density and porosity of the samples were estimated by the hydrostatic method in accordance with ISO 27.38.2009.

The morphology of the starting powders and the microstructure of the sintered materials were studied using optical (Olympus LX-70) and scanning electron (TESCAN VEGA) microscopes. The phase composition of the materials was determined on a Dron-3M diffractometer in Co-Kα radiation. The sample during shooting rotated around its axis.

Local X-ray spectral analysis was carried out using an X-ray microprobe MS-46 from CAMECA (France). A quantitative analysis of the composition of the phases under study was made at points under the probe mode, an accelerating voltage of 20 kV, and a probe diameter of 0.7 μm. The concentrations were calculated using the ZOND program [9], which was modernized according to the features of this work, which takes into account the above correction for absorption, fluorescence, and the atomic number of the element.

The microhardness of the structural components was determined on a PMT-3 device using a load of 0.49 N, and the strength properties of the material were determined using an INSTRON 8802 testing machine.




a b

Fig. 1. Morphology of the starting powders of iron (a) and ferrochrome (b)

**RESULTS AND DISCUSSION**

According to the micro X-ray diffraction analysis, high-carbon ferrochrome in a lump state consists of two phases (Fig. 2): double iron-chromium carbide with the composition: 10 % Fe - 80.6 % Cr - 8.9 % C (wt.) (Phase 1), and an iron-chromium-carbon alloy containing 72.7 % Fe - 22.3 % Cr - 4.8 % C (wt.) (Phase 2).

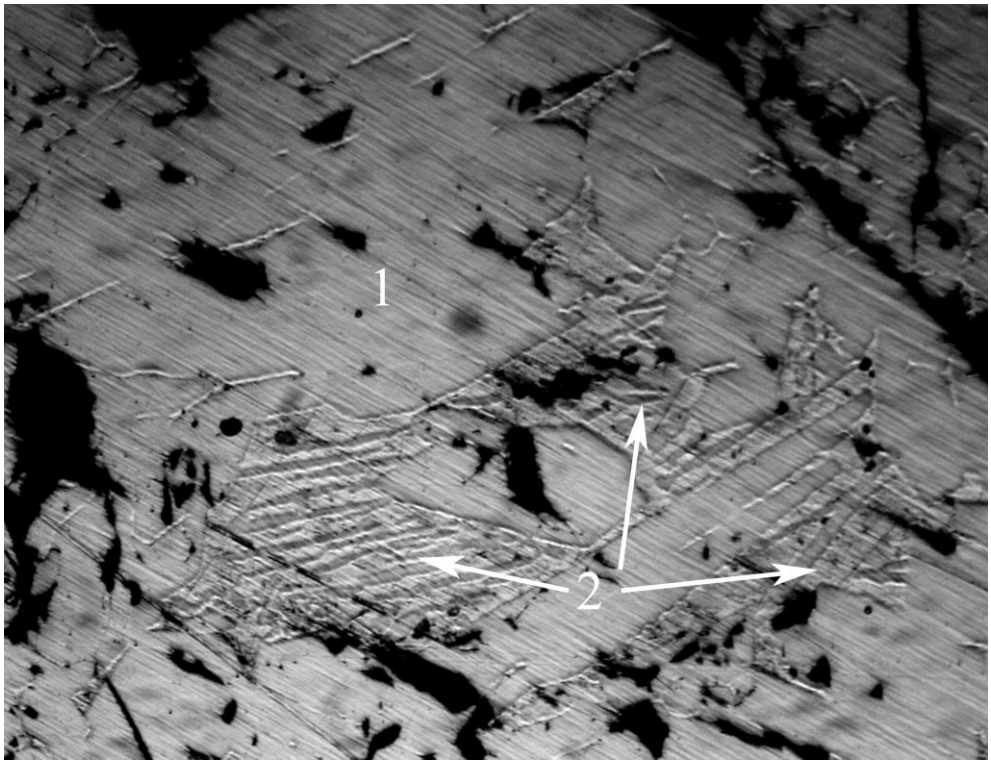



Fig. 2. The microstructure of the initial ferrochrome

The X-ray diffraction pattern analysis identified the phase composition of ferrochrome powder, which is presented by two main phases: $(Cr, Fe)_7C_3$ carbide and a solid solution of chromium in α-Fe. In addition to the main $(Cr, Fe)_7C_3$ carbide component, weak intensity lines of $Cr_3C_2$, $Cr_7C_3$ carbides as well as $Cr_{23}C_6$ with insufficient stoichiometry were detected, which is obviously due to the partial replacement of chromium by iron in $Cr_{23}C_6$ carbide (Fig. 3).

Significant tailing of the (110) reflection of the ferritic phase indicates its nonequilibrium state, which is confirmed by the calculated values of the fine structure parameters. It was found that the physical broadening of (110) reflection is β110 = 14,5 mrad, and the dispersion of the coherent scattering regions (CSR) is 15 nm.

The analysis of estimation of sintering temperature effect on structure and properties of sintered materials results showed that sintering at temperatures of 1000÷1100 °C practically does not lead to shrinkage of the samples, while at the temperature of 1000 °C even some increase is observed (up to 1.5%) due to the Frenkel effect, which manifests

itself in the difference in the values of the heterodiffusion coefficients of chromium and iron in the powder mixture during sintering.

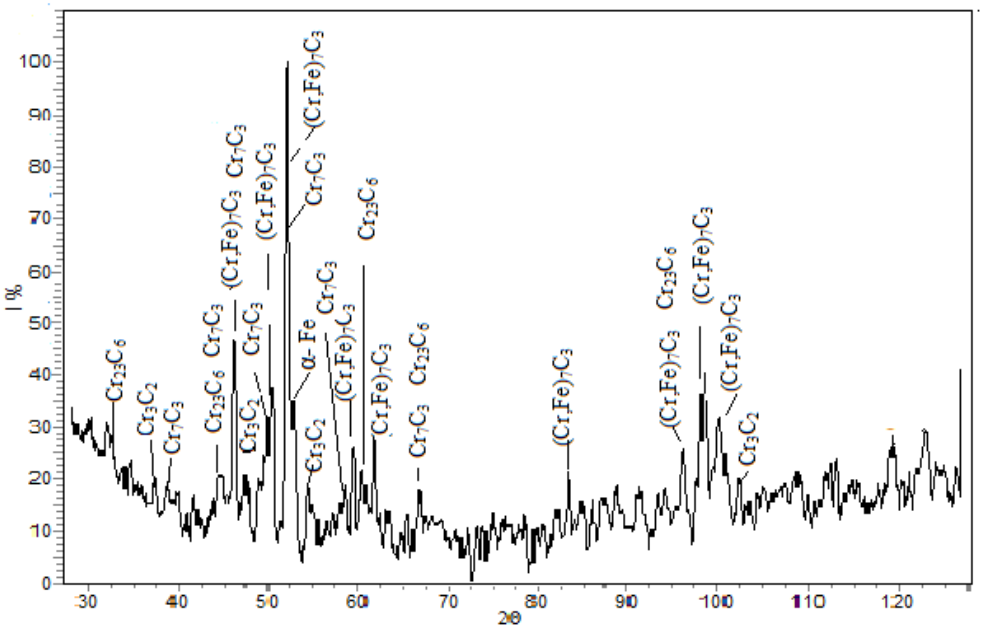



Fig. 3. The XR diffraction pattern of the ferrochrome powder

Slightly noticeable shrinkage of the samples occurs only at temperatures above 1150 °C, however, even sintering at 1200 °C does not provide samples of the material with minimal porosity. Only an increase in temperature up to 1250 °C allows obtaining samples with porosity not exceeding 2 %, while its increase to 1300 °C leads to partial melting and shape distortion of the samples.

The microstructure of the composite sintered at 1250 °C is essentially heterogeneous and consists of 2 predominant phases: dark gray, which is a double ferrochromium carbide, and a light gray metal component. A small number of pores (black) is observed on the microsection too (Fig. 4).

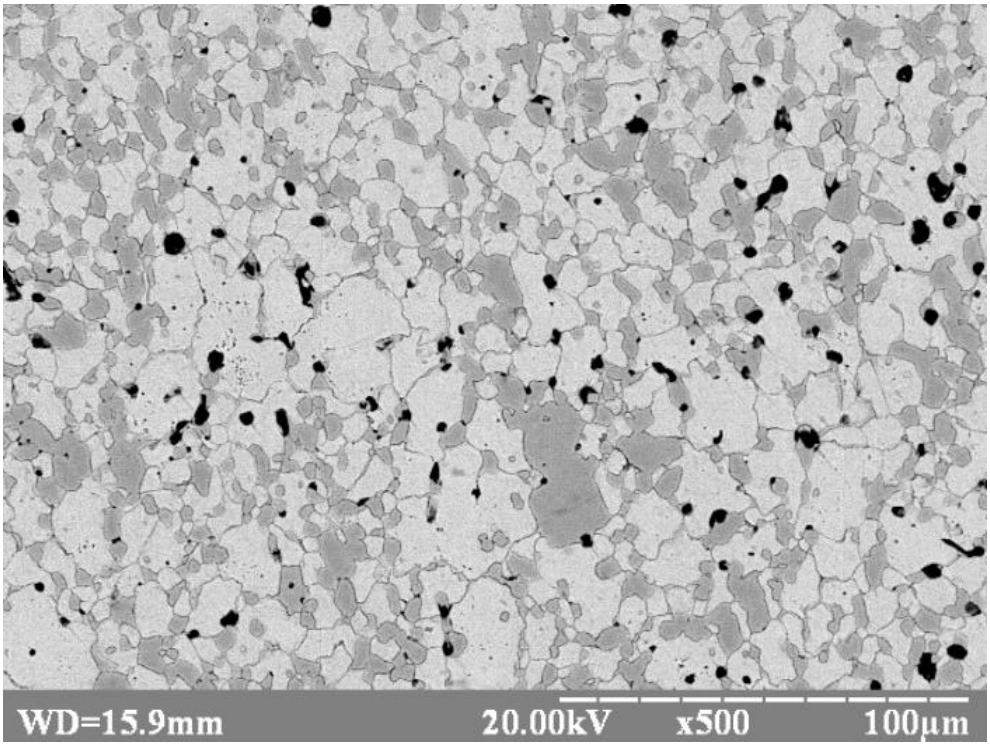



Fig. 4. The microstructure of the composite, sintered at 1250 °C

The estimation of the effect of sintering temperature on the microhardness of the matrix and main carbide phases of sintered composite (Fig. 5) made it possible to reveal the following regularities. With the increase of sintering temperature monotonic increase of matrix phase hardness is observed due to the thermally activated process of carbide transformations in the iron-ferrochrome system by the mechanism of chromium and carbon atoms diffusion from the main carbide phase of $M_7C_3$ of ferrochrome into iron and counter flow of iron atoms to ferrochrome.

At the same time, the depletion of ferrochrome particles by chromium and carbon occurs, resulting in a sharp decrease in the microhardness of its carbides in the temperature range of 1000-1100 °C. However, with a further increase in sintering temperature to 1200–1250 °C, the reverse tendency is observed to increase in the microhardness of the secondary carbide phase formed based on the matrix phase.

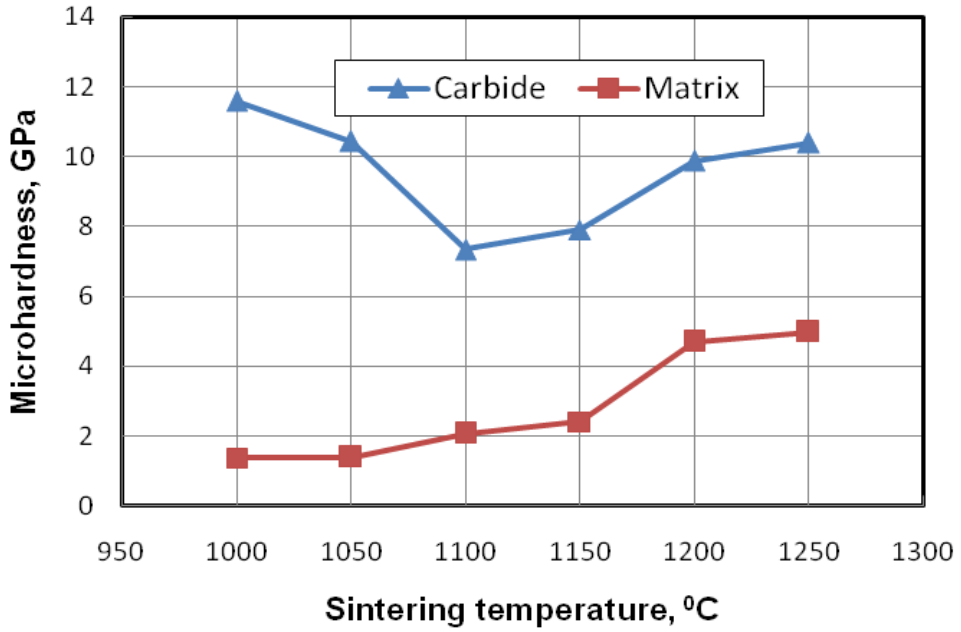



Fig. 5. The dependence of the carbide and matrix phases microhardness on the sintering temperature.

To establish the mechanism of this phenomenon, X-ray microspectral studies of the composition of the carbide phase of the composite sintered at different temperatures were carried out. According to these results (Tab. 1), sintering of compacts from a mixture of iron and ferrochrome powders in the low-temperature region leads to a certain decrease in the carbon content of the carbide phase from the initial 8.0 % (in ferrochrome) to 6.6÷7,1 % (wt.) after sintering at temperatures 1050÷1150 °C. At the same time, its atomic content decreases from 27.6 % to 25.1÷23.8 %, and the ratio $C_c/C_m$ for atomic content of carbon (Cc) and metal (Cm) component of carbides decreases from 0.38 (in ferrochrome) to 0.31÷0.33. The data presented indicate the probability of execution of phase transformation of the initial carbide $M_7C_3$ from ferrochrome, into $M_3C$.

Tab. 1. The effect of sintering temperature on elemental and phase composition of the carbide phase

| t, $^0$C | The content of elements in the carbide phase, % (mass./atomic) | | | $C_c/C_m$ | Phase |
|---|---|---|---|---|---|
| | Fe | Cr | C | | |
| 20 | 69,2 /55,4 | 22,9 /17,1 | 8,0 /27,6 | 0,38 | $M_7C_3$ |
| 1000 | 70,8/58,4 | 22,3 /17,1 | 6,9 /24,5 | 0,32 | $M_3C$ |
| 1050 | 68,1 /56,6 | 25,3 /19,6 | 6,6 /23,8 | 0,31 | $M_3C$ |
| 1100 | 68,3 /56,1 | 24,7 /18,9 | 7,1 /25,1 | 0,33 | $M_3C$ |
| 1150 | 68,4 /56,2 | 24,6 /18,8 | 7,1 /25,1 | 0,33 | $M_3C$ |
| 1200 | 67,7 /53,1 | 23,6 /17,2 | 8,8 /29,7 | 0,42 | $M_7C_3$ |
| 1250 | 67,4 /52,1 | 23,5 /16,4 | 9,1 /31,5 | 0,46 | $M_7C_3$ |

With the increase of sintering temperature to 1200-1250 °C, the diffusion intensity of chromium and carbon atoms from the main carbide phase of ferrochrome to iron increases, which becomes the basis for the formation of a new, secondary $M_7C_3$ carbide phase. This fact is confirmed by the increase to 0.42÷0.46 of the value of the $C_c/C_m$ ratio corresponding to the $M_7C_3$ type carbide phase.

The above results allow us to present the mechanism of dissolution of ferrochrome in the iron matrix as the following sequence: at the first stage, in the temperature range of 1000–1150 °C at the interaction of ferrochrome particles with iron one-way diffusion of chromium and carbon from ferrochrome particles to iron occurs. It is accompanied by depletion of $M_7C_3$ carbides located as a part of ferrochrome, by carbon and their conversion to $M_3C$ carbides. With an increase of sintering temperature to 1200–1250 °C in consequence of recrystallization, new (secondary) $M_7C_3$ carbides with a hexagonal lattice are formed in the alloy structure.

X-ray phase analysis of the composite sintered at 1250 °C showed (Fig. 6) that the most intense lines are fixed on the X-ray diffraction pattern, indicating the predominant presence of double carbide $(Cr, Fe)_7C_3$ in the composition. The peaks of the $Cr_7C_3$ and $Cr_3C_2$ carbide phases, γ-Fe and α-Fe are noted in the X-ray diffraction pattern too. It should be noted that γ-Fe and α-Fe reflections, partially overlap with $(Cr, Fe)_7C_3$ lines.

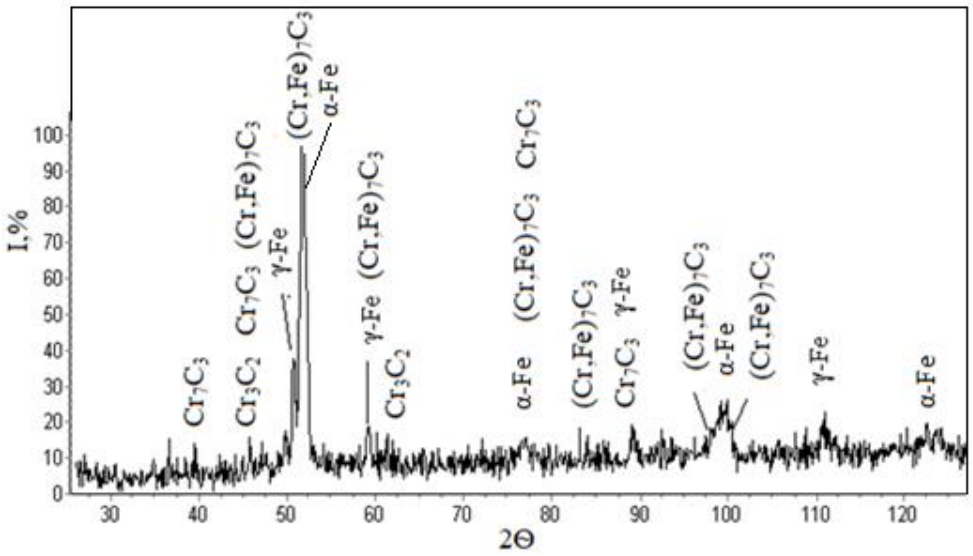



Fig. 6. The XR diffraction pattern of a sample sintered at 1250 °C

It can be assumed that during sintering of the mixture of iron and ferrochrome powders, part of the carbon from the carbide phase of high-carbon ferrochrome dissolves in Fe to form an austenitic phase.

The calculations of the fine structure parameters of the Fe matrix from the (111) and (311) profiles revealed a defect in the crystal lattice of the austenitic phase. Thus, the broadening of (111) line is β111 = 4.7 mrad, CSR = 29 nm. Profile (311) is characterized by broadening of β311 = 9.17 mrad, microdistortions of the crystal lattice within 9.0*10-2, and a dislocation density of ρ = 1.7*1012 cm-2.

Tab. 2 shows the effect of sintering temperature on the Fe-35% FX800 properties. From the given data it can be seen that with an increase in the sintering temperature from 1100 to 1250 °C, the density of the samples monotonically increases, and the porosity decreases accordingly. The sintering temperature has a significant effect on the hardness of the composites and their bending strength. As can be seen from Tab. 2, with an increase in the sintering temperature to 1250 °C, the hardness and bending strength in the samples reach maximum values. This is explained both by a significant increase in sample density (decrease in porosity) and a possible strengthening of the adhesion bond at the carbide-metal matrix boundaries as a result of the more active interaction of the components. The best combinations of density, minimum porosity, and maximum hardness and bending strength of composites are observed at a sintering temperature of 1250 °C. The composite sintered at 1250 °C with a porosity of about 1.5÷2.5 % has a hardness of HRA 74÷75 and bending strength of 1760÷1900 MPa.

Tab. 2. The effect of sintering temperature on Fe-35% (Fe-Cr) properties

| t,°C | γ, g/cm$^3$ | Porosity, % | HRA | Bending strength, MPa |
|---|---|---|---|---|
| 1100 | 7,1÷7,12 | 4,2÷4,4 | 55÷57 | 900÷1100 |
| 1150 | 7,14÷7,19 | 3,2÷3,9 | 68÷69 | 1150÷1280 |
| 1200 | 7,2÷7,22 | 2,8÷-3 | 71÷72 | 1550÷1670 |
| 1250 | 7.25÷7,3 | 1,5÷2,5 | 74÷75 | 1760÷1900 |

## CONCLUSIONS

1. It is shown using the results of X-ray phase and X-ray diffraction pattern analyses, that during sintering of compacts from a mixture of iron powders and high-carbon ferrochrome, the components of the mixture actively interact with the formation of substantially heterogeneous structure.
2. The phase composition of sintered alloy includes the metal component which is a solid-solution austenitic phase and predominant content of double $(Cr, Fe)_7C_3$ carbide.
3. The mechanism for dissolving of ferrochrome in the iron matrix is proposed as the following sequence: unilateral diffusion of chromium and carbon from ferrochrome particles to iron → depletion of $M_7C_3$ carbides with their conversion to $M_3C$ carbide (at 1000÷1150 $^0$C) → formation of secondary $M_7C_3$ carbides with hexagonal lattice in consequence of recrystallization (at 1200÷1250 $^0$C).

## REFERENCES

[1] Fedorchenko, IM., Frantsevich, IN., Radomyselsky, ID., et al.: Powder metallurgy, materials, technology, properties, applications: Handbook. Kyiv: Nauk. Dumka., 1985, 624. (In Russian).
[2] Baglyuk, GA., Poznyak, LA.: Powder Metall. Met. Ceram., vol. 40, no. 1, 2001, p. 34–39.
[3] Lu, L., Soda, H., McLean, A.: Mater. Sci. Eng. A., vol. 347, Issues 1–2, 2003, p. 214-222.
[4] Herranz, G., Matula, G., Romero, A.: Powder Metallurgy. vol. 60, Issue 2, 2017, p. 120–130.
[5] Chang, CM., Chen, YC., Wu, W.: Tribol. Int., vol. 43, isses 5-6, 2010, p. 929–934.

[6] Yakovenko, RV., Maslyuk, VA., Mamonova, AA., Gripachevskii, AN., Denisenko, NI.: Powder Metall. Met. Ceram., vol. 52, 2014, p. 644–650.
[7] Yakovenko, RV., Maslyuk, VA., Gripachevskii, AN., Deimontovich, VB.: Powder Metall. Met. Ceram., vol. 50, 2011, p. 182–188.
[8] Tolochin, AI., Laptev, AV., Yakovenko, RV., Maslyuk, VA.: Powder Metall. Met. Ceram., vol. 55, 2017, p. 518–529.
[9] Tsikunov, NS., Batyrev, VA., Gripachevskii, AN. et al. A software package for processing the results of quantitative X-ray spectral microanalysis using the ZAF method on a mini-computer. Kyiv: Institute of Metallophysics, Academy of Sciences of the Ukrainian SSR. 1981, p. 40. (In Russian).